

Experimental study of the growth of liquid ^4He films on graphite

S. Kumar, T. Brosius, G. Torzo,* D. Finotello, and J. D. Maynard

Department of Physics, The Pennsylvania State University, University Park, Pennsylvania 16802

(Received 27 June 1987; revised manuscript received 25 September 1987)

We report experiments with superfluid ^4He films physisorbed on graphite which indicate a continuous growth of the film up to at least 25 layers. The growth of the film is monitored by the decreasing third-sound resonance frequency of an annular resonator made out of graphite fibers; such a resonator overcomes problems of capillary condensation and interference from ordinary sound in the helium vapor. Measurements have been performed from 1.25 K to as low as 0.35 K.

I. INTRODUCTION

The study of physisorbed films has attracted the attention of a large number of workers in the past decade.¹⁻¹² Such films have provided a basis for extensive theoretical¹⁻⁴ and experimental⁵⁻¹² work directed towards an understanding of the nature of physical processes such as two-dimensional phase transitions, film growth, and wetting. The growth of a film on a substrate and its wetting behavior depend on the relative strengths of the substrate-atom and the atom-atom interactions. Different types of film growth have been experimentally observed using a variety of techniques. If the substrate-atom interaction is relatively strong in comparison with the atom-atom interaction, the film completely wets the substrate resulting in the type-1 mode of film growth. If the substrate-atom interaction is relatively weak the film usually exhibits non-wetting or partially wetting characteristics leading to the type-2 mode of film growth. However, a series of papers by Dash and his co-workers⁹⁻¹² discussing experiments done with various adsorbates on uniform well-characterized substrates (such as graphite and noble metals) have reported partial or incomplete wetting for adsorbates which are under the influence of a strong attractive potential of the graphite substrate. Dash characterizes this type of growth as reentrant type-2 growth; intermediately strong attraction between the substrate and the adsorbate leads to complete wetting, but stronger attraction leads to the adsorbate reentering the incomplete wetting mode of film growth.

This reentrant incomplete wetting may be explained by the fact that relatively strong lateral variations are present with a strong substrate potential which can create a lattice constant and/or symmetry mismatch between the adsorbate and the substrate if the adsorbed film is solidlike. This mismatch inhibits the growth of the film beyond a few layers. This explanation is consistent with current theories¹⁻⁴ on multilayer growth and wetting, and has been described in a more precise theory by Huse.⁴ However, because of its quantum nature, helium layers other than the first few are liquid. Different experiments have indicated different wetting behavior for ^4He on graphite. The quantum nature of helium may play a role in its wetting behavior.

The experiments showing evidence of incomplete wetting of ^4He on graphite have involved measurements on porous and exfoliated graphite materials which have a complicated and tortuous internal geometry. Crevices present in such materials could very well act as sites for capillary condensation leading to the formation of bulk liquid. The growth of the bulk liquid formations inhibits the growth of the film. There is no easy way to distinguish the formation of the bulk on the film as a consequence of partially wetting behavior from the formation of bulk due to capillary condensation. Theoretical calculations¹³ of the onset of capillary condensation agree with experimental observations which indicate that the film is limited to a thickness of four to seven layers depending on the nature of the substrate. One of the ways to avoid capillary condensation is to use nonporous graphite materials which have a simpler geometry. Two examples of such materials are highly oriented pyrolytic graphite (HOPG) and graphite fibers. Before discussing the use of these materials in a wetting experiment, our method of measurement should first be described.

The presence of superfluidity in helium films permits the use of third sound to probe the film. Third sound is a surface wave in a superfluid film whose velocity is given by¹⁴

$$c_3^2 = \frac{\rho_s}{\rho} d \frac{\partial V}{\partial d} \simeq \frac{\rho_s}{\rho} \frac{3\alpha}{d^3}, \quad (1)$$

where C_3 is the third-sound velocity, ρ_s/ρ is the average superfluid fraction in the film, V is the van der Waals potential, α is the van der Waals force constant, and d is the film thickness. Third sound probes wetting behavior through its dependence on film thickness. A major advantage is that, in the case of incomplete wetting, third sound only propagates in the thin-film part of the adsorbed system and is relatively unaffected by the formation of bulk droplets. Thus, if the film stops growing, then the third-sound speed becomes constant. By contrast, microbalance measurements measure loading continuously whether the additional mass is in the film or in bulk droplets. The analysis of third sound to determine wetting behavior will be further discussed in the concluding section of this paper.

We have used third-sound techniques to study wetting

on a graphite substrate and have found steady growth of the film at temperatures as low as 0.35 K to thicknesses higher than those which have been reported so far. These experiments have involved the use of graphite fibers as both the substrate and as the ballast in the experimental cell; graphite fibers being nonporous help avoid capillary condensation of helium in the cell. The use of an acoustic resonator has enabled precise measurements of the third-sound resonance frequency (which is directly proportional to the third-sound velocity), while avoiding interference from the ordinary sound in the helium vapor which is usually present in time-of-flight measurements of the third-sound velocity. The film thickness has been monitored independently by simultaneous measurements of the third-sound velocity on glass, a substrate for which there is extensive data.

II. REVIEW OF EARLIER RESULTS

Early measurements¹⁵ of third sound on exfoliated graphite (Grafoil) foam were made to test the Kosterlitz-Thouless-Nelson^{16,17} theory of superfluid onset for ^4He films on a uniform substrate. The same experiments also showed oscillations of the third-sound velocity as a function of film thickness. Other measurements¹⁸ on HOPG revealed similar behavior, but with even larger oscillations; the period of the oscillations was about one atomic layer, as illustrated in Fig. 1. This behavior contrasted with the smooth decrease of the third-sound speed with increasing film thickness on substrates such as glass, and suggested the possibility of discrete layering in the helium film on atomically uniform substrates. The motivation, apart from its nonporosity, in using HOPG was the availability of relatively large ($\sim 10\,000 \text{ \AA}^2$) domains of atomic uniformity. This uniformity is necessary to ensure that the physical phenomena such as layering are not obscured by the presence of variations in α , grain boundaries, and other defects.

The experiments done with the HOPG further indicated that the oscillations of the third-sound velocity become more pronounced as the temperature is lowered. The lower limit of the temperature at the time of this experiment was 1 K. Due to the presence of grafoil foam as ballast in the experimental cell, film thicknesses greater than six or seven layers could not be obtained because of

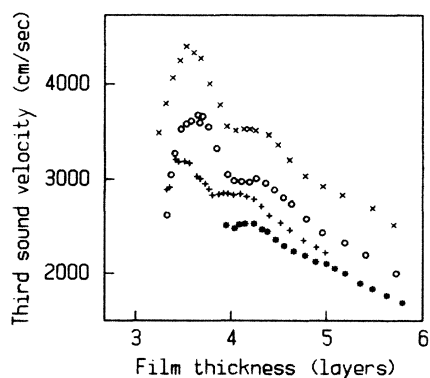


FIG. 1. Third sound on HOPG, from Ref. 18.

the onset of capillary condensation in the grafoil foam.

The main motivation for the experiment reported here was to determine how thick the ^4He film would continuously grow on a uniform graphite substrate. The nature of this growth on graphite would provide a limit for the wetting nature of ^4He on graphite. It is also expected that effects of the wetting behavior are usually more pronounced at lower temperatures. The layering of the ^4He film as suggested by the earlier experiment on HOPG was of additional interest. Predictions of large oscillations¹⁹ in the third-sound velocity at low temperatures, and the evidence of layering of solid ^4He on graphite,⁸ added to the motivation in obtaining lower temperature data for liquid ^4He on graphite. A ^3He cryostat was constructed to achieve temperatures lower than 1 K.

III. THE GRAPHITE FIBER RESONATOR

Initial attempts at obtaining the data below 1 K involved time-of-flight measurements on HOPG. However, the third-sound signals obtained suffered from interference with the vapor sound reflections present in the cell. This problem seemed to become more acute at lower temperatures. Damping of the vapor sound would have called for lining the walls of the cell with some sound absorbing material, such as cotton, to prevent vapor sound reflections, and the relatively tedious procedure of the placement of a shield around the HOPG sample between the drive heater and the pickup bolometer to limit the direct vapor sound wave.

The use of an annular resonator is advantageous due to the fact that while the third-sound signal in the film is amplified by the Q of the resonator, the vapor sound is not; hence the effects of the vapor sound are rendered negligible. HOPG was perceived as not a good substance for fabricating an annular resonator because of limitations in the available size and its flaky nature which make it difficult to handle. By contrast, graphite fibers, which are commercially available, are suitable for the construction of an annular resonator. Results of other experiments,²⁰ and electron micrographs,²¹ indicate that properly treated graphite fibers have good atomic uniformity.

The graphite substrate used consisted of fibers manufactured by Union Carbide,²² whose average diameter is ten micrometers, which were baked at about 450°C for six hours in a hydrogen atmosphere to clean their surfaces. The third-sound generator, which is a heater, is made up of about 15 cm of $1640 \Omega/\text{m}$ Evanohm wire. The heater wire was folded over a number of times at the middle to form a bundle about 1 cm long leaving single lengths of wire at each end. The heater was then mounted on a 5-cm-long by 3-cm-wide by $25\text{-}\mu\text{m}$ -thick Mylar strip by attaching the bundle at the middle to the sticky side of a small piece of Teflon pressure sensitive tape which was itself mounted on the Mylar strip. The third sound sensor is a bolometer which is a 2.5-cm-long, 0.3-cm-wide piece of aluminized Mylar whose middle section ($\sim 2 \text{ mm}$ in length), is narrowed down to 0.25 mm, thereby forming the active sensing area. The bolometer was mounted on the Mylar strip in a fashion similar to the heater. The distance between the bolometer and the

heater was set approximately to be half the circumferential length of the annulus (further discussed herein).

A 1.25-cm-diameter Teflon rod was mounted horizontally in a fixture which permitted the rotation of the rod about its axis. The Mylar strip, with the heater and the bolometer, was wrapped around the rod with the heater and the bolometer parallel to its axis and diametrically opposite one another. One end of a bundle of about 100 graphite fibers 1 m long was then positioned near the heater with a piece of tape. The other end was attached to a weight which provided some tension. The rod was then rotated slowly about its axis and the fiber bundle was guided to wrap with moderate tension around the middle sections of the heater and the bolometer. After the completion of four or five complete rotations, resulting in a corresponding number of closely spaced loops of the fibers, small pieces of Teflon tape were mounted across the fibers at the positions of the heater and the bolometer so as to stick to the pieces of tape already under them. The remaining length of the bundle was then cut off. The Mylar strip was then slipped off the rod along with the loops of fiber and, subsequently, the loops of fiber were slipped off the strip. The free-standing loops of fiber form the annulus of the resonator.

Because the graphite fibers in the resonator bundle touch one another, especially in the regions where the transducers are taped, one might wonder if capillary condensation is still a problem. In exfoliated graphite materials, including the more open "foam," the crevices are spaced on the order of the pore sizes, in the range 0.01–1.0 μm . Microscopic examination of the graphite fiber resonator shows that the fibers are fairly parallel and loosely packed, touching at intervals on the order of 1 mm, thus giving a significantly smaller density of capillary condensation sites. The site density may be higher in the regions of the transducers, but these regions comprise only $\sim 5\%$ of the total resonator circumference, and thus cannot affect the resonant frequency by more than a few percent. Furthermore, the results of the experiment confirm that capillary condensation is not a problem; the reasoning is as follows.

If the experiment had shown that at some point the

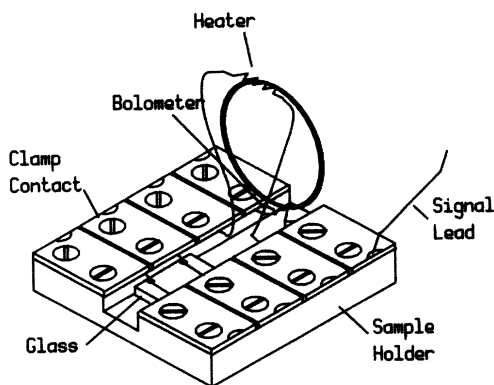


FIG. 2. Bakelite holder for the graphite fiber resonator and the glass substrate. Only one copper clamp has been shown connected to a wire.

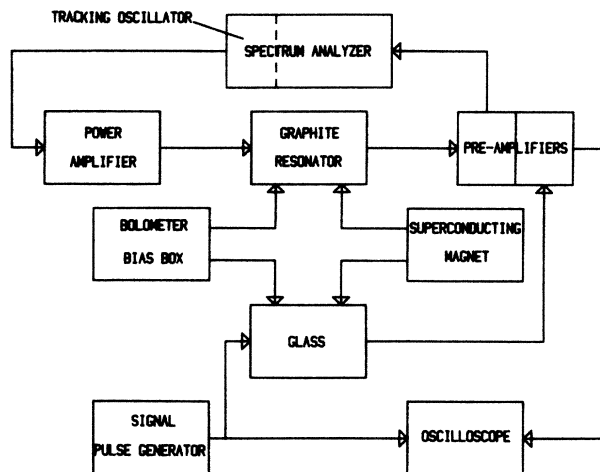


FIG. 3. Block diagram of the electronics for third-sound production and detection.

third-sound speed had ceased to decrease as more helium was added, then one would require evidence as to whether the effect was due to capillary condensation or incomplete wetting. However, the experiment showed that the third-sound velocity continued to decrease, and the conclusion is that, at least to the thicknesses where the third-sound signal was observable, there was neither significant capillary condensation nor incomplete wetting; either of these phenomena would have caused the third-sound velocity to depart significantly from its normal trend.

The graphite fiber resonator, as shown in Fig. 2, was mounted on a bakelite holder with the help of two 30-gauge copper wires around which the two ends of the heater wire were wound. A touch of silver epoxy ensured good electrical contacts between the heater and the copper wires. The copper wires were then clamped down to the holder with copper clamps. The bolometer was also clamped at each end with a little indium to improve contact to the copper clamps.

The equipment used to monitor the third sound is illustrated in Fig. 3. A spectrum analyzer was used as a tracking oscillator to measure the resonance frequency. The output from the tracking oscillator was fed through a power amplifier to the heater on the resonator.

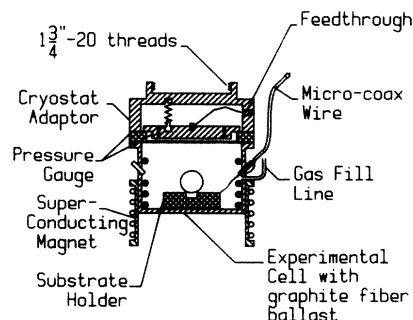


FIG. 4. The experimental setup which attaches to the ^3He cryostat.

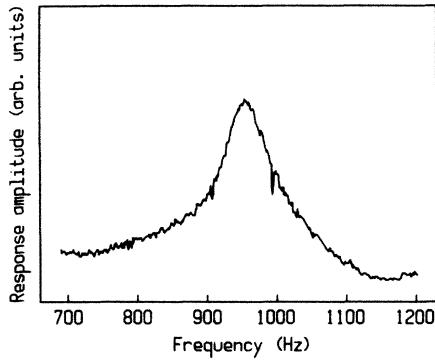


FIG. 5. Typical third-sound resonance peaks obtained with the graphite fiber resonator. In this particular instance the temperature was 0.8 K and the film thickness was approximately four layers.

Standing-wave resonances created around the loop of graphite fibers were detected with the aluminum bolometer. The bolometer was biased at the superconducting transition at the experimental temperature with the help of a dc bias current and a magnetic field created by a superconducting magnet attached to the copper cell (see Fig. 4).

The actual performance of the resonator is excellent in terms of the output resonance signal. A typical resonance signal is shown in Fig. 5. Frequency shifts of a few hertz are easily measured and therefore the small changes in film thicknesses (tenths of a layer) are easily detected.

IV. OTHER EXPERIMENTAL APPARATUS AND PROCEDURE

As stated previously, an independent measure of the helium-film thickness was obtained by measuring the third-sound velocity on glass to complement the third-sound measurements on graphite. The film thickness could also have been obtained using the estimate of the surface area of the cell including the substrate and the ballast obtained from an *in situ* adsorption isotherm with nitrogen at 77 K. However, the absence of any porous form of graphite in the cell greatly reduces the surface area, a large surface area being preferred for a good isotherm. The use of porous materials was avoided to prevent the film growth being inhibited due to capillary condensation. The measurement of the vapor pressure in the experimental cell could also have been used to determine the film thickness by making use of the Frenkel-Halsey-Hill²³ relation. Due to the low temperatures and the low pressures involved, this measurement would have had to be made by a gauge in the cell itself to eliminate thermo-molecular effects. A beryllium-copper diaphragm gauge was constructed and attached to the experimental cell (as shown in Fig. 4) with the intent of estimating the film thickness with both the glass third-sound data and the cell vapor pressure if necessary. However, the glass data were found to be adequate for interpreting the graphite data.

The speed of third sound on glass provides a way to in-

dependently obtain a value for the film thickness on the graphite if one accounts for the difference in the van der Waals constant between glass and graphite. The availability of extensive third-sound data on glass substrates,^{24,25} and the usual high quality of the third-sound signal on glass, led to the choice of glass as the control substrate. The system to measure the third-sound velocity on glass was fabricated using a 1-cm square piece of glass which was cut out of a clean microscopic slide on which two parallel thin strips of aluminum, 8 mm apart, were evaporated. Copper wires indium soldered to the ends of these strips were made to contact copper clamps on the holder as shown in Fig. 2. The aluminum strips can act as either third-sound generators (heaters) or sensors (bolometers). A time-of-flight measurement was used to measure the third-sound speed on the glass. Pulses which were generated by a signal generator (shown in Fig. 3) were fed to one of the aluminum strips which acted as a heater. Third-sound pulses thus generated were sensed by the other aluminum strip which acted as a bolometer. The time-of-flight was measured with an oscilloscope. This, along with the known separation between the strips, was used to determine the third-sound speed.

The bakelite holder resides in the experimental cell (shown in Fig. 4) which is attached to the ^3He pot of the ^3He cryostat. The inside of the cell is ringed with graphite fibers to act as a ballast surface for adsorbed helium film. Electrical connections from the cell to the cryostat are made with microcoaxial cables.

The gas handling system consists of a 0.6-m-long section of 0.4-mm stainless-steel capillary leading from the cell to the 4-K stage of the ^3He refrigerator and thermally anchored to the various stages on the way. A length of 1.5-mm thin walled stainless-steel tube completes the gas fill line to the top of the cryostat. A set of small bellows valves control access to the ^4He gas reservoir of known volume and a MKS Baratron (Ref. 26) 100 torr pressure sensing head. By monitoring the decreasing reservoir pressure as gas is added to the cell, the precise dosing (expressed in units of torr cm^3) of ^4He may be determined.

The experimental cell is cooled down to the required temperature by the ^3He cryostat before any ^4He gas is added. Purified ^4He gas is added very gradually until third sound appears, indicating the onset of superfluidity in the ^4He film. The resonance frequency of the third sound on the graphite is continually monitored by adding measured amounts of gas equivalent to about a tenth of a layer. The third-sound speed on the glass is measured periodically. Measurements were made along isotherms at temperatures from 1.25 K down to 0.35 K.

V. RESULTS OF THIS EXPERIMENT

The raw data obtained consists of the amount of ^4He gas added into the experimental cell from the metering volume and the corresponding third-sound resonance frequencies on graphite and times-of-flight on glass for a number of temperatures. The glass data obtained at each temperature are analyzed using the traditional $d^{-3/2}$ dependence for the third-sound speed as a function of

film thicknesses indicated in Eq. (1). It should be noted that for thick films Eq. (1) is only approximate. At 20–25 layers the van der Waals potential must be corrected by about 25%;²⁷ however, the correction to d determined from the rightmost part of Eq. (1) is in error by only $\sim 7\%$. The reason for the reduced discrepancy is that determining d involves the cube root, and that the third-sound speed involves the derivative of the van der Waals potential. For thin films there is another correction which arises from the fact that the superfluid component density in a film is not the same as that in the bulk, but is modified to include both the effects of the presence of a few solid layers next to the substrate, and the effect due to the boundary conditions present at the film-substrate and the film-vapor interface. The superfluid component density in the film may be written as

$$\frac{\rho_s^{\text{film}}}{\rho} = \frac{\rho_s^{\text{bulk}}}{\rho} \left[1 - \frac{D}{d} \right], \quad (2)$$

where D is an effective healing length obtained from Ref. 24. It is this density that is used in Eq. (1).

Figure 6 shows the graphite third-sound resonance frequency versus the nominal film thickness obtained from the glass substrate data; the resonances for a given isotherm have been shifted by a constant to facilitate plotting in a single figure. By comparing this figure with the data for third sound on HOPG in Fig. 1, it can be seen that layering oscillations are much weaker on the graphite fibers than on the HOPG. This may be due to an unaccounted for lack of sufficient resolution in the experiment, but we believe instead that it is due to a lack of graphite platelets on the fibers which are large in the lateral as well as axial direc-

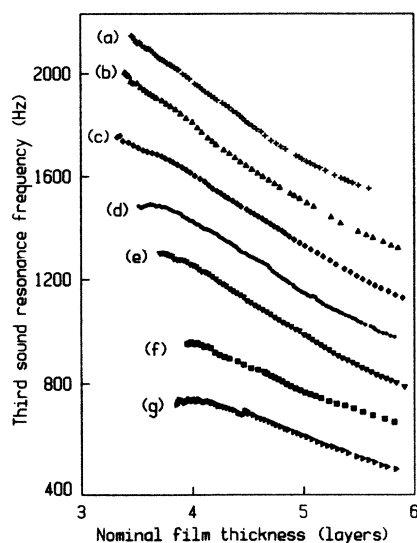


FIG. 6. Third-sound resonance frequency vs nominal film thickness obtained from the glass substrate data at various temperatures. To facilitate plotting, the data for each isotherm are shifted upward by a constant. The temperatures and associated shifts are as follows: (a) 0.35 K, 1050 Hz; (b) 0.40 K, 850 Hz; (c) 0.70 K, 700 Hz; (d) 0.80 K, 500 Hz; (e) 0.90 K, 300 Hz; (f) 1.10 K, 200 Hz; (g) 1.15 K, 0 Hz.

tions. This is evident in electron micrographs of the fibers which show long but very narrow sections on the fiber surface; this is in contrast to HOPG which has micrometer scale uniformity in two dimensions. It is possible that, graphitizing the fibers at temperatures ($\sim 2000^\circ\text{C}$) much higher than the 450°C which we used for cleaning, would greatly improve the ability to observe discrete layering as on the HOPG.

Our most significant results are presented in Fig. 7, which is a plot of nominal film thickness on the graphite fibers determined from the third-sound resonance versus the amount of ^4He added to the cell. The conversion from third-sound resonance to film thickness is based on the $d^{-3/2}$ dependence and is normalized with the data from the glass substrate (i.e., with the data in Fig. 6) using the values of $\alpha = 27 \text{ layers}^3\text{-K}$ for glass and $\alpha = 44 \text{ layers}^3\text{-K}$ for graphite.¹⁵ The different data sets in Fig. 7 are for different isotherms: 0.35, 0.75, and 1.25 K. The last data point (the highest nominal film thickness) for each isotherm represents the point at which the large attenuation of third sound precludes continued precise measurement. The important feature of the data is that the rate of film growth with the amount of gas added remains finite up to the point at which third sound can no longer be measured. If there were incomplete wetting then the plots in Fig. 7 would become horizontal, or at least approach horizontal, but there is no suggestion of such behavior in the figure. The major advantage of third sound is that it is sensitive to the thinnest parts of the adsorbed system, because of the $d^{-3/2}$ dependence. If the film stops growing, then the third-sound speed should become nearly constant. If additional ^4He is added and bulk droplets form, then the third sound may be somewhat decreased because of an acoustic scattering correction. However, there is a limit as to how much this can effect the third-sound speed, with the result that if there is incomplete wetting, then the slopes of the plots in Fig. 7 would have to decrease by more than a factor of 4 at the onset of droplet formation. (A theoretical derivation of this result is presented in the Appendix.) A qualitative example of droplet formation starting at ~ 16 lay-

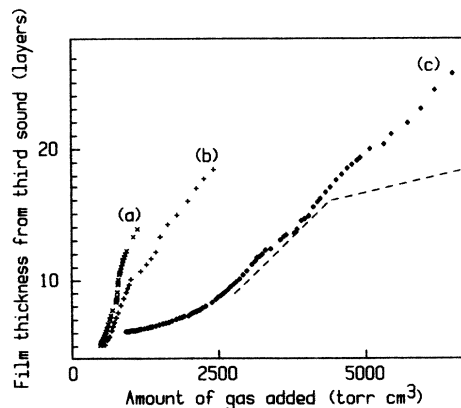


FIG. 7. Nominal film thickness from the graphite third-sound resonance vs the amount of ^4He added for various temperatures. (a) 0.35 K; (b) 0.75 K; (c) 1.25 K.

ers is given by the dashed line in Fig. 7; the section above ~ 16 layers is an upper bound for the effects of the droplets. As there is no evidence of this behavior, we conclude that the film continues to wet the graphite, down to temperatures as low as 0.35 K.

At the lower temperatures the data in Fig. 7 show some variations in slope at intermediate coverages, 8–10 layers. We believe this is not due to variations in the third-sound speed, but rather is due to changes in the relationship between the amount of gas added (from outside the cryostat) and the amount of ^4He which actually becomes adsorbed on the graphite. As the vapor pressure above the adsorbed film increases, more ^4He goes into the vapor phase in the cell and some may become capillary condensed in other (possible higher temperature) parts of the cryostat. The most important point, clearly evident in Fig. 7, is that as more ^4He is added to the cell, the speed of third sound, proportional to $d^{-3/2}$, monotonically decreases at the highest coverages, indicating complete wetting.

These results strongly suggest that liquid ^4He completely wets graphite down to temperatures of 0.35 K. There seems to be no evidence of bulk droplet formation as suggested by Bienfait *et al.*⁹ Results published recently by Taborek and Senator²⁸ also seem to indicate that superfluid ^4He wets graphite, although their experiments suggest that normal ^4He does not.

ACKNOWLEDGMENTS

We would like to thank M. H. W. Chan, M. W. Cole, and J. G. Dash for helpful discussions. This research was supported by National Science Foundation (NSF) Grants No. DMR-83-04371 and No. DMR-87-01682, and in part by the U.S. Office of Naval Research.

APPENDIX

In the case of incomplete wetting, the helium-film thickness remains constant at some value d_0 , and any helium subsequently added goes into the growth of droplets. While the third sound in the helium film remains at a constant speed given by

$$C_0^2 \simeq (\rho_s/\rho)3\alpha/d_0^3,$$

the third-sound waves may be scattered by the droplets so that the experimentally measured speed C_3 is reduced from C_0 by an acoustic "index of refraction" n defined by

$C_3 = C_0/n$. As more helium is added and droplets grow in size, n increases and C_3 decreases, even though C_0 remains constant. In this appendix we establish an upper limit for the change in C_3 due to the acoustic scattering.

In order to relate these results to the data presented in Fig. 7, we define the "film thickness" determined from third sound as

$$d' = (3\alpha\rho_s/\rho)^{1/3}C_3^{-2/3}. \quad (\text{A1})$$

For the case of complete wetting $d' = d$, and when ΔN moles of helium are added to N moles already in a wetting film, we have

$$\Delta d'/d' = \Delta N/N, \quad (\text{A2})$$

which would produce straight lines in Fig. 7. For incomplete wetting

$$d' = (3\alpha\rho_s/\rho)^{1/3}C_0^{-2/3}n^{2/3}. \quad (\text{A3})$$

For a worst case prediction one assumes that the droplets act as perfect scatterers. For the scattering theory we assume two-dimensional waves scattering from random circular obstacles; in this case $n^2 = (2-P)$, (Ref. 29) where P is the fraction of the substrate covered by film (not covered by droplets). If there are N moles of helium in bulk (three-dimensional) droplets, then the area covered by the droplets is proportional to $N^{2/3}$, and

$$(2-P) = (1 + \beta N^{2/3}),$$

where β is some constant which depends on the droplet geometry and density. Now when ΔN moles of helium are added, we have from Eq. (A3)

$$\frac{\Delta d'}{d'} = \frac{2}{9} \frac{\beta N^{2/3}}{(1 + \beta N^{2/3})} \frac{\Delta N}{N} < \frac{2}{9} \frac{\Delta N}{N}. \quad (\text{A4})$$

Comparing this with Eq. (A2), we see that in the case of incomplete wetting d' changes with N at a rate less than 2/9ths of the rate in the case of complete wetting. This behavior is indicated qualitatively by the dashed line in Fig. 7, with droplet scattering starting at ~ 16 layers; more realistic acoustic scattering by the droplets would produce an even sharper break in the dashed line. If there were incomplete wetting so that the film thickness became constant, then C_3 would become nearly constant, and there would be a clear break in the d' versus N curves in Fig. 7.

*Permanent address: Istituto di Fisica Galileo Galilei, Università degli Studi di Padova, via Marzolo 8, I-35100 Padova, Italy.

¹M. J. de Oliveira and R. B. Griffiths, *Surf. Sci.* **71**, 687 (1987).

²C. Ebner and W. F. Saam, *Phys. Rev. Lett.* **38**, 1486 (1977).

³R. Pandit, M. Schick, and M. Wortis, *Phys. Rev. B* **26**, 5112 (1982).

⁴D. A. Huse, *Phys. Rev. B* **29**, 6985 (1984).

⁵S. K. Satija, L. Passell, J. Eckert, W. Ellenson, and H. Patterson, *Phys. Rev. Lett.* **51**, 411 (1983).

⁶J. W. Schmidt and M. R. Moldover, *J. Chem. Phys.* **79**, 379 (1983).

⁷D. D. Awschalom, G. N. Lewis, and S. Gregory, *Phys. Rev. Lett.* **51**, 586 (1983).

⁸S. Ramesh and J. D. Maynard, *Phys. Rev. Lett.* **49**, 47 (1982); S. Ramesh, Q. Zhang, G. Torzo and J. D. Maynard, *Phys. Rev. Lett.* **52**, 2375 (1984).

⁹M. Bienfait, J. G. Dash, and J. Stoltenberg, *Phys. Rev. B* **21**, 2765 (1980).

¹⁰M. Bienfait, J. L. Sequin, J. Suzanne, E. Lerner, J. Krim, and

- J. G. Dash, *Phys. Rev. B* **29**, 983 (1984).
- ¹¹J. Krim, J. G. Dash, and J. Suzanne, *Phys. Rev. Lett.* **52**, 640 (1984).
- ¹²A. D. Migone, J. Krim, and J. G. Dash, *Phys. Rev. B* **31**, 7643 (1985).
- ¹³M. W. Cole (private communication); see also M. W. Cole and W. F. Saam, *Phys. Rev. Lett.* **32**, 985 (1974).
- ¹⁴S. J. Putterman, *Superfluid Hydrodynamics* (North-Holland, Amsterdam, 1974), pp. 212–234.
- ¹⁵J. A. Roth, G. J. Jelatis, and J. D. Maynard, *Phys. Rev. Lett.* **44**, 333 (1980).
- ¹⁶J. M. Kosterlitz and D. J. Thouless, *J. Phys. C* **6**, 1181 (1973).
- ¹⁷D. R. Nelson and D. J. Kosterlitz, *Phys. Rev. Lett.* **39**, 1201 (1977).
- ¹⁸J. D. Maynard and M. H. W. Chan, *Physica* **110B**, 2090 (1982).
- ¹⁹R. D. Puff and J. G. Dash, *Phys. Rev. B* **21**, 2815 (1980).
- ²⁰C. E. Bartosch and S. Gregory, *Phys. Rev. Lett.* **54**, 2513 (1985).
- ²¹D. J. Johnson, in *Chemistry and Physics of Carbon*, edited by P. L. Walker and P. A. Thrower (Dekker, New York, 1987), Vol. 20, p. 1.
- ²²Union Carbide Corporation, Carbon Products Division, 120 South Riverside Plaza, Chicago, IL 60606.
- ²³ $d = [(T/\alpha) \ln(P_0/P)]^{-1/3}$ where the symbols have the usual meanings; for a review, see W. A. Steele, *The Interaction of Gases with Solid Surfaces* (Pergamon, Oxford, 1974), pp. 221–269.
- ²⁴J. C. Fraser, Ph.D. thesis, University of California at Los Angeles, 1969; J. H. Scholtz, Ph.D. thesis, University of California at Los Angeles, 1973. See also J. H. Scholtz, E. O. McLean, and I. Rudnick, *Phys. Rev. Lett.* **32**, 147 (1974). The constant B in this paper is incorrect by a factor 2.172 (T_λ); the correct value is $B = 2.45$.
- ²⁵J. E. Rutledge, W. L. McMillan, J. M. Mochel, and T. E. Washburn, *Phys. Rev. B* **18**, 2155 (1978); J. S. Brooks, F. M. Ellis, and R. B. Hallock, *Phys. Rev. Lett.* **40**, 240 (1978).
- ²⁶MKS Instruments, Inc., 22 Third Avenue, Burlington, MA 01803.
- ²⁷From E. S. Sabisky and C. H. Anderson, *Phys. Rev. A* **7**, 790 (1973), $V(d) = \alpha/[d^3 f(d)]$, where $f(d) = [1 + Bd(d+c)]^{1/2}$, with $B \simeq 8.4 \times 10^{-5} \text{ \AA}^{-2}$ and $c \simeq 132 \text{ \AA}$.
- ²⁸P. Taborek and L. Senator, *Phys. Rev. Lett.* **57**, 218 (1986).
- ²⁹D. L. Johnson and P. N. Sen, *Phys. Rev. B* **24**, 2486 (1981).